Research Statement

Chartese Jones

1 Current Project:

As I embark on the journey to absorb more about the mathematical world, I continue to find new channels and pathways that uncover the secrets of the world around us. This has become further evident with some of my contemporary compositions. These compositions encompass solid and liquid tumors elimination. In this work, via chaos control, a virtual laboratory is utilized to understand the dynamical behavior and inner connectedness of solid and liquid tumors in the process of eradication. From clinical data and research, mathematical models and algorithms are developed and formulated to uncover the precise importance of these phenomena. With these virtual laboratories, we preserve all possible outcomes, and in many cases eradicate such problems all together. In the exploration of clinical data, Chimeric Antigen Receptor T (CAR-T)–cell immunotherapy for immunodeficient mice therapy of hematological cancers response depends on the following factors:

1. Capacity of CAR-T cells to kill tumor cells.
2. The formulation of long-term immunological memory.
3. Immunosuppressive effects of the tumor microenvironment.

After the approval of CAR T cell therapies in 2017 by the Federal Drug Administration, immunotherapy attracted more recognition. This procedure can be initiated when an individual's/patient's T lymphocytes are genetically altered to identify tumor-specific antigens. This process helps with minimizing tumor growth and possibly tumor remission. However, there is still a challenge in CAR-T cell immunotherapy and all cellular therapies, which is the exhaustion of implanted cells. To investigate this occurrence, we look to a mathematical model of CAR-T immunotherapy in pre-clinical studies of Hematological cancers. Luciana R. C. Barros et. at. [11] , constructed a mathematical model that explored the back-and-forth amongst tumor cells, effector CAR-T cells, and memory CAR-T cells. In their work, the authors built a three-population mathematical model to describe tumor response to CAR-T cell immunotherapy in immunodeficient mouse models, encompassing interactions between a non-solid tumor and CAR-T cells. Their model is composed of ordinary differential equations (ODEs). We present their model,

$$\left\{\begin{array}{rcl} \frac{dC_T}{dt} &=& \phi C_T - \rho C_T + \theta T C_M - \alpha T C_T \\ \frac{dC_M}{dt} &=& \epsilon C_T - \theta T C_M - \mu C_M \\ \frac{dT}{dt} &=& rT(1-bT) - \gamma C_T T. \end{array}\right. \tag{1}$$

In the above model, T, C_T, and C_M, represent tumor cells, effector CAR-T cells, and memory CAR-T cells, respectively.

With the following equations, $C_T = \frac{r}{\gamma}X, C_M = \frac{r}{\gamma}Y, T = \frac{1}{b}Z$, and $t = \frac{1}{r}\tau$, the following dimensionless system is obtained from system (1),

$$\begin{cases} X' &= -pX + qZY - sZX \\ Y' &= uX - qZY - wY \\ Z' &= Z(1-Z) - XZ. \end{cases} \tag{2}$$

To extremely investigate the correlations of this model, the total effect of effector CART-cell must be observed. For this purpose, we specifically explore the dynamics of the effector (activated) CART- cells for system (1),

$$\frac{dC_T}{dt} = \phi C_T - \rho C_T + \theta T C_M - \alpha T C_T.$$

With this richer assessment, using biological nuances, the stimulatory/inhibitory signals on effector CART-cells transformed by the tumor are where we start our investigation. In system (**??**), we will study the stability of the non-trivial equilibrium points. We will also study Hopf Bifurcation of the system, which results in a periodic solution. We will give the stability of the periodic solution by calculating the first Lyapunov coefficient. Finally, we will give a numerical example to illustrate our results.

For example, we will investigate the dynamic behavior of Hopf bifurcation stability. We study this behavior because oscillatory contours are frequently observed throughout nature. Many have argued and shown the importance and strength that this line of research. To tackle the shortcomings, We are interested in the special case when s converges to zero ($s \to 0$). In the absence of s, the CART-cells have now become ineffective in their ability to arouse or repress the tumor cells..

We now propose the new dimensionless system of ordinary differential equations for CAR-T cell therapy with numerical simulations to demonstrate the steadiness of the anew purported structure,

$$\begin{cases} X' &= -pX + qZY \\ Y' &= uX - qZY - wY \\ Z' &= Z(1-Z) - XZ. \end{cases} \tag{3}$$

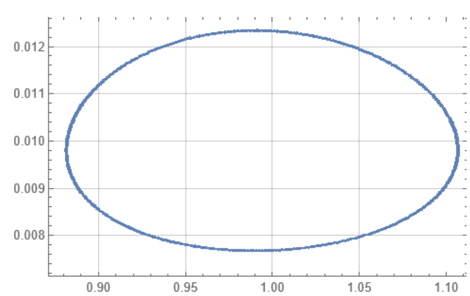

Figure 1: Limit Cycle: Numerical Result for Stability

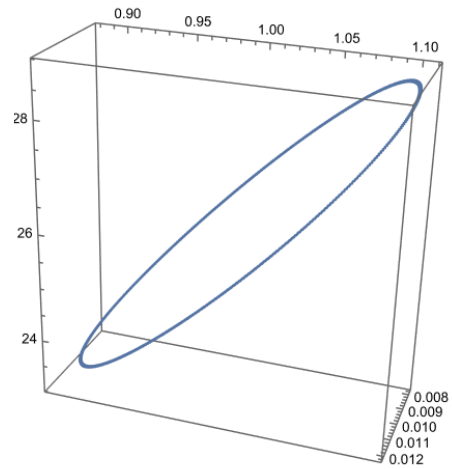

Figure 2: 3D Limit Cycle: Numerical Result for Stability

2 Published Article(s):

We have developed several denoising methods and their associated algorithms based on TV and NLM for speckle noisy images. Speckle noise is mostly present in ultrasound images, synthetic aperture radar (SAR) images, or acoustic images. It is granular in nature, and it exists inherently in the images. Unlike Gaussian noise, which affects single pixels of an image, speckle noise affects multiple pixels. The noise is multiplicative, whereas Gaussian noise is additive. Hence, it is not possible to remove speckle noise with the traditional gaussian denoising models.

1. Edge Enhancing Accelerated Diffusion (EEAD) Model

Krissian *et al.* [6] suggested the following speckle noise equation:

$$f = u + \sqrt{u}n, \tag{4}$$

where u is the desired image to fine, n is Gaussian noise, and f is the observed image. Hence using $n = \frac{f-u}{\sqrt{u}}$, the general regularized minimization functional is given as :

$$\inf_u F(u), \quad F = \int_\Omega \left[|\nabla u| + \frac{\lambda}{2}\left(\frac{f-u}{\sqrt{u}}\right)^2 \right] d\mathbf{x}. \tag{5}$$

The time marching non-linear PDE which is asscoiated with the corresponding Euler Lagrange equation is

$$\frac{\partial u}{\partial t} - \frac{u^2}{f+u}|\nabla u|\nabla \cdot \left(\frac{\nabla u}{|\nabla u|}\right) = \lambda|\nabla u|(f-u). \tag{6}$$

This method can accelerate the diffusion process and therefore remove noise quickly. However, the uniform diffusion over the region does not incorporate the specific regions of interest - noisy regions. This may lead to an oversmoothing effect. In 2019, we have developed the following noise equation

[9] for speckle denoising:

$$f = u + \sqrt{u + C|u - f_s|^{\alpha}} \cdot n. \tag{7}$$

Here, f_s denotes the smoothed version of the given observed image f. By adopting the non-convexity of the minimizing functional in [5] for edge enhancement and by using the strategy developed by Marquina and Osher [8] to prevent the staircasing effect, the following Edge Enhancing Accelerated Diffusion (EEAD) model has been proposed:

$$\frac{\partial u}{\partial t} = (u + C|u - f_s|^{\alpha})|\nabla u|^{2-p} \nabla \cdot \left(\frac{\nabla u}{|\nabla u|^{2-p}} \right) + \lambda |\nabla u|^{2-p}(f - u), \quad 0 < p < 1. \tag{8}$$

An explicit numerical scheme for our EEAD model following the linearized time stepping procedure [2] has been developed and the stability of the scheme under a certain condition on Δt has been proved in [9]. The EEAD algorithm was tested to several images with synthetic or natural speckle noise and the results were compared to the ones using the Krissian *et al.* model. All of the images showed that EEAD produces more accurate results than the Krissian *et al.* model.

	Krissian *et al.*		EEAD	
	Time (s)	PSNR	Time (s)	PSNR
Block (PSNR=28.03)	2.85	30.05	3.68	32.57
Lenna (PSNR=25.70)	2.88	28.23	3.63	30.01
Gallstone	4.06	–	5.19	–
Liver	2.83	–	3.64	–

(a) (b) (c)

Figure 3: Liver: (a) Original, (b) Krissian *et al.*, (c) EEAD

2. Quarter Match Non-Local Means Algorithms for Noise Removal

The standard non-local means (NLM) method [1] is very accurate in removing noise compared to other conventional denoising methods. However, the main drawback is on computational inefficiency due to its non-locality. To overcome the drawback, the authors of [4] suggested the use of blocks B_{i_k} of size $(2\alpha + 1)^2$ with overlapping supports and performed NLM restoration on these blocks instead of pixels. The following is the proposed formula to restore images:

$$NL[u](B_{i_k}) = \sum_{B_j \in V_{i_k}} w(B_{i_k}, B_j) u(B_j) \tag{9}$$

with

$$w(B_{i_k}, B_j) = \frac{1}{Z_{i_k}} e^{-\frac{||u(B_{i_k}) - u(B_j)||_2^2}{\hat{h}^2}}, \tag{10}$$

where Z_{i_k} is a normalization constant ensureing that $\sum_{B_j \in V_{i_k}} w(B_{i_k}, B_j) = 1$ and $\hat{h}$ is a smoothing parameter. Since blocks are simultaneously updated, this blockwise NLM method significantly reduced the computation time for the NLM method. Inspired by Mahmoudi and Sapiro [7] who proposed a method to preselect the most similar neighborhoods only to avoid unneccessary weight computation, we have developed several NLM blockwise selective algorithms for speckle noise images.

Average gradient The weight $w(B_{i_k}, B_j)$ was only considered when the ratios of average gradients of $u(B_{i_k})$ and $u(B_j)$ are within a sufficiently small range around 1. Here the average gradient is denoted by

$$\overline{\nabla \mathfrak{v}}(i) = (\overline{\mathfrak{v}_x}(i), \overline{\mathfrak{v}_y}(i)), \tag{11}$$

where $\mathfrak{v}(i)$ and $\mathfrak{v}(j)$ represents the gray values in the neighborhood of pixels i and j.

Angles between neighborhoods The weight was selected only when the angles between the two neighborhoods were sufficiently small. To measure the angle between two neighborhoods $\mathfrak{v}(i)$ and $\mathfrak{v}(j)$, the following equation was used:

$$\cos(\theta) = \frac{\overline{\nabla \mathfrak{v}}(i) \cdot \overline{\nabla \mathfrak{v}}(j)}{||\overline{\nabla \mathfrak{v}}(i)|| \; ||\overline{\nabla \mathfrak{v}}(j)||}. \tag{12}$$

This method was developed to prevent the possibility of neighborhoos having the similar mean and angles but not similar at all. Examples of this:

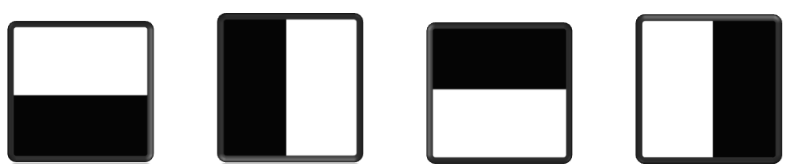

We minimized this issue by dividing each of our blocks into four parts to compare the average of each of those quarters with other neighborhoods.

(a) (b) (c)

All of selective blockwise NLM methods were numerically tested and compared to the original and blockwise NLM. The new methods are still accurate enough and more efficient than the original and blockwise NLM filter.

Figure 4: Lenna: (a) Original, (b) Speckle Noisy, (c) Quarter selective $h = 125$

3 Algorithm Devloped: Article Formulation- Research Continuation

Chambolle Accelerated Diffusion (CAD) Model

BACKGROUND

Gray scale images can be expressed as a two variable function defined on a rectangular domain. We denote an original noise free image by u and an observed noisy image by f. Hence $u, f : \Omega \subset \mathbb{R}^2 \to \mathbb{R}$. In general, an observed image f is represented by the equation:

$$f = u + n, \tag{13}$$

where n is the Gaussian noise. For a denoising model, the main objective is to reconstruct u from an observed image f. In 1992, Rubin, Osher, and Fatemi [10] proposed the total variation (TV) denoising model as the minimization problem:

$$\inf_u F(u), \quad F = \int_\Omega |\nabla u| d\mathbf{x} + \frac{\lambda}{2} \int_\Omega (f-u)^2 d\mathbf{x}. \tag{14}$$

Applying an evolution parameter t to the corresponding Euler Lagrange equation gives the TV Gaussian denoising model as:

$$\frac{\partial u}{\partial t} - \nabla \cdot \left(\frac{\nabla u}{|\nabla u|} \right) = \lambda (f - u). \tag{15}$$

The TV model is computationally efficient on denoising images corrupted by Gaussian noise but it produces staircasing effect [5]. In [5], Kim and Lim introduced a nonconvex diffusion model to prevent the staircasing effect and to enhance edges:

$$\frac{\partial u}{\partial t} - |\nabla u|^{2-p} \nabla \cdot \left(\frac{\nabla u}{|\nabla u|^{2-p}} \right) = \lambda |\nabla u|^{2-p} (f-u), \quad p \in (0,1). \tag{16}$$

Besides the PDE based models, some filtering based techniques were also proved to be very precise in removing noise and preserving texture of images. Among them the most remarkable results were observed for the non-local means (NLM) method [1]. The method is given by the formula

$$NL(u)(\mathbf{x}) = \frac{1}{C(\mathbf{x})} \int e^{-\frac{(G_a * |u(\mathbf{x}_{+.}) - u(\mathbf{y}_{+.})|^2)(0)}{h^2}} u(\mathbf{y}) d\mathbf{y}, \tag{17}$$

where G_a is a Gaussian Kernel with standard deviation a, $C(x) = \int e^{-\frac{(G_a * |u(\mathbf{x}_{+.}) - u(\mathbf{z}_{+.})|^2)(0)}{h^2}} d\mathbf{z}$ is the normalizing factor, and h acts as a filtering parameter. The NLM method estimates the value of $\mathbf{x}$ as a weighted average of the values of all the pixels in the entire image. Due to non-locality and the weighted averaging technique with the similar neighborhoods, the NLM method is very accurate in removing noise. However, the main drawback is on computational complexity.

In [3], Chambolle proposed a fast projection algorithm for minimizing the TV functional in [10]. He obtained the equivalent dual problem as

$$\min_{|p_{i,j}| \leq 1} \frac{1}{2} \|\mathbf{div} p - \frac{f}{\lambda}\|^2, \tag{18}$$

where $\mathbf{div} p = w$ for $p = (p_{i,j}); i, j = 1, \ldots, N \in Y = XxX$ and $w = \frac{f-u}{\lambda}$. The following algorithm was proposed to update p:

$$p_{i,j}^{n+1} = \frac{p_{i,j}^n + \tau(\nabla(\mathbf{div} p^n - \frac{f}{\lambda}))_{i,j}}{1 + \tau(|(\nabla(\mathbf{div} p^n - \frac{f}{\lambda}))_{i,j}|}. \tag{19}$$

Due to its simpler dual formation, the method is more efficient than the original TV model. However, it is not suitable for speckle denoising. Using the modified version of EEAD noise equation (7), we propose the following form of a noise equation:

$$f = u + (\sqrt{f + C|f - f_s|^\alpha})n \tag{20}$$

which gives

$$\min_u F(u), \quad F(u) = \lambda J(u) + \frac{1}{2} \int_\Omega \frac{(u - f)^2}{\beta} d\mathbf{x}, \tag{21}$$

where

$$J(u) = \int_\Omega |\nabla u| d\mathbf{x}, \qquad \beta = f + C|f - f_s|^\alpha. \tag{22}$$

One can show that the Euler Lagrange equation for the minimizing functional (21) is

$$\partial J(u) + \frac{u - f}{\lambda \beta} \ni 0. \tag{23}$$

4 Path Forward:

Furture Plans

We are currently working on combining Chamoblle model with efficiency and Non-local means model with accuracy. Our new research requires new definitions as classical derivates are local operators.

Minimization functional:

$$\inf_u F(u) = \int_\Omega |\nabla_{NL} u| + \frac{\lambda}{2}(u - u_0)^2 dx \tag{24}$$

Minimizing, Euler Lagrange gives the model as:

$$u_t = \int_\Omega w(x,y)(u(y) - u(x))\Big(|\nabla_{NL} u|^{-1}(x) + |\nabla_{NL} u|^{-1}(y)\Big) - \lambda(u(y) - u(x))dy \tag{25}$$

$\Omega \subset \mathbb{R}^n, x \in \Omega, u : \Omega \to \mathbb{R}, w(x,y) =$ weights between points x and y. Consider $w(x,y) = w(y,x)$.

- NL vectors: Mappings $p : \Omega\ x\ \Omega \to \mathbb{R}$.
- NL gradient: $\nabla_{NL} u(x,y) = (u(y) - u(x))\sqrt{w(x,y)}$
- NL norm: $|p|(x) = \sqrt{\int_\Omega p(x,y)^2 dy}$
- NL divergence: $div_{NLl} p(x) = \int_\Omega (p(x,y) - p(y,x))\sqrt{w(x,y)}dy$

5 Collaborative Research:

Modeling and quantifying the effect of blood pressure, intraocular pressure, and blood viscosity on the central retinal artery hemodynamics in people of European and African descent [12, 13]

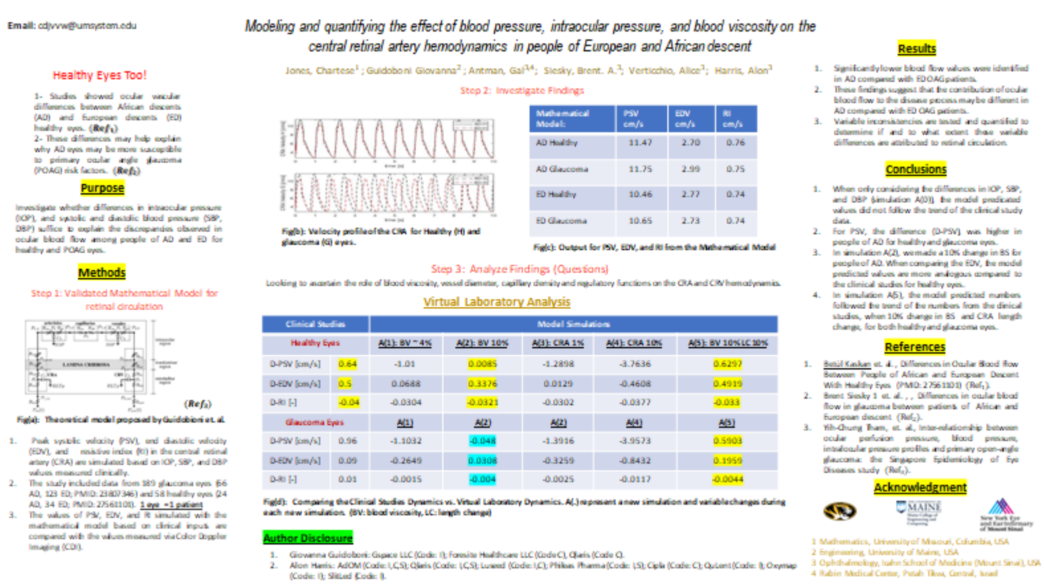

Figure 5: Jones, Chartese; Guidoboni Giovanna; Antman, Gal; Siesky, Brent. A.; Verticchio, Alice; Harris, Alon

References

[1] A. Buades, B. Coll, and J. M. Morel. Nonlocal image and movie denoising. *International Journal of Computer Vision*, 76(2):123–139, 2008.

[2] Y. Cha and S. Kim. Edge-forming methods for image zooming. *J. Math. Imaging Vision*, 25:353–364, 2006.

[3] A. Chambolle. An algorithm for total variation minimization and applications. *J. Math Imaging Vision*, pages 89–97, 2004.

[4] P. Coupe, P. Yger, S. Prima, P. Hellier, C. Kervrann, and C. Barillot. An optimized blockwise non local means denoising filter for 3-d magnetic resonance images. *IEEE Transctions on Medical Imaging*, 27(4):425–441, 2008.

[5] S. Kim and H. Lim. A non-convex diffusion model for simultaneous image denoising and edge enhancement. *Electro. J. of Diff. Eq.*, 15:175–192, 2007.

[6] K. Krissian, R. Kikinis, C.-F. Westin, and K. Vosburgh. Speckle-constrained filtering of ultrasound images. *in Proc. IEEE Computer Society Conf. Computer Vision and Patter Recognition, Sand Diego CA*, 2:547–552, Jun. 2005.

[7] M. Mahmoudi and G. Sapiro. Fast image and video denoising via nonlocal means of similar neighborhoods. *IEEE Signal Processing Letters*, 12(12):839–842, 2005.

[8] A. Marquina and S. Osher. Explicit algorithms for a new time dependent model based on level set motion for nonlinear deblurring and noise removal. *SIAM J. Sci. Comput*, 22:387–405, 1999.

[9] A. B. Misra, C. Jones, and H. Lim. Edge enhancing accelerated diffusion model for speckle denoising in medical imagery. In *Proceedings of the 1st International Conference on Computational Methods and Applications in Engineering (ICCMAE 2018)*, Timisoara, Romania, May 23-26, 2018. in press.

[10] L. I. Rudin, S. Osher, and E. Fatemi. Nonlinear total variation based noise removal algorithms. *Physica D*, 60:259–268, 1992.

[11] Luciana R. C. Barros. Emanuelle A. Paixão, Andrea M. P. Valli, Gustavo T. Naozuka, Artur C. Fassoni, and Regina C. Almeida. CARTmath—A Mathematical Model of CAR-T Immunotherapy in Preclinical Studies of Hematological Cancers. *Cancers*, 13(12):2941, 2021.

[12] Brent Siesky, Alon Harris, Alice Verticchio Vercellin, Julia Arciero, Brendan Fry, George Eckert, Giovanna Guidoboni, Francesco Oddone, and Gal Antman. Heterogeneity of Ocular Hemodynamic Biomarkers among Open Angle Glaucoma Patients of African and European Descent *Clinical Medicine*, 12(4):1287, 2023.

[13] Guidoboni G, Harris A, Cassani S, Arciero J, Siesky B, Amireskandari A, Tobe L, Egan P, Januleviciene I, and Park J. Intraocular pressure, blood pressure, and retinal blood flow autoregulation: a mathematical model to clarify their relationship and clinical relevance. *Ophthalmol Vis Sci*, 55(7):4105-4118, 2014.